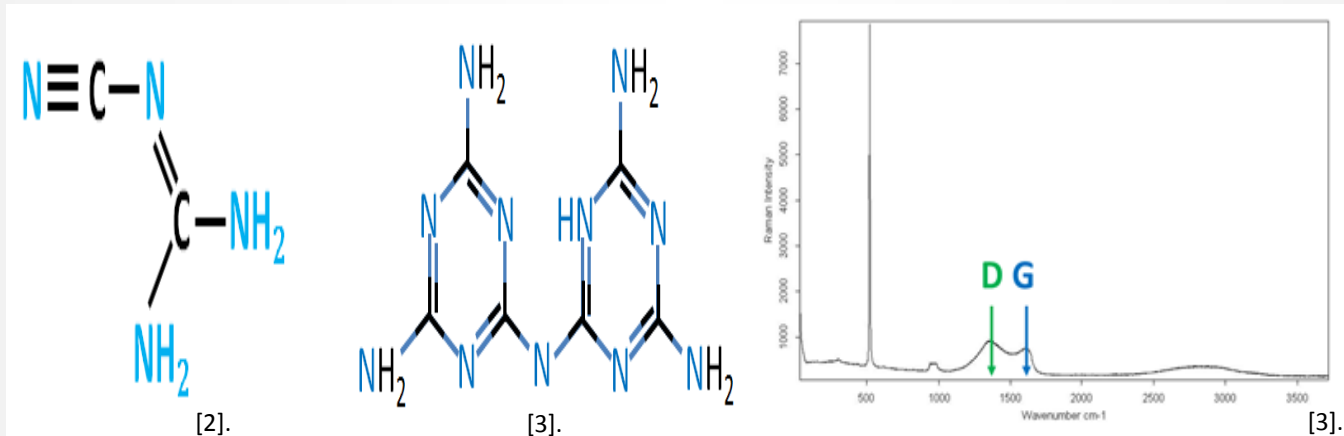


GROWTH OF SINGLE LAYER THIN FILMS OF GRAPHITIC CARBON NITRIDE A 2-D SEMICONDUCTOR MATERIAL USING CVD



Abdul M. Syed, Michael M. Masaki, Caitlin M. DragunBianchi and Joel M. Therrien
Nanomanufacturing Center of Excellence (NCOE)
William J. Kennedy Jr. Nanotechnology Research & Development Center
Sensors, Photonics & Integrated Nanomaterials (SPIN) Lab, Mark & Elisia Saab ETIC
and
ECE Department at UMass Lowell

Presenter: **Abdul M. Syed**

Agenda/Outline

□ Part I: Background and Motivation

- 2D materials, properties, applications and structure
- Synthesis method for 2D materials
- Characterization of 2D material

□ Part II: CVD growth process of single layer film of carbon nitride

- Thermogravimetric study of Dicyandiamide (Dicy)
- Mass loading curve of Dicy w.r.t temperature *versus* TG of Dicy under dry nitrogen atmosphere and TGA of Melamine
- Results by [3]
- Proposed design for gas delivery system for controlled CVD growth

□ Part III: Conclusion

- Device Applications using 2D materials & Future Work
- Acknowledgement & References

Part I

Background and Motivation

□ 2D materials

- From Butler et al. [4]

- A material in which atomic organization and bond strength along two dimensions are similar & much stronger than along a third dimension.
- Single layer materials: Are 2D crystalline materials consisting of single layer of atoms.

□ Properties of 2D materials

- Reduced dimensionality and symmetry leading to phenomena different from bulk material.
- Has high specific surface areas (Since entirely made up of surface & interface between surface, substrate & presence of adatoms, defects alter the inherent material properties).
- Layer dependent property changes – Transformation of band structure as single layer is approached (Tuning electronic properties by surface manipulation).
- 2D nature plays a mechanical role as they are inherently flexible, strong & extremely thin.
- Unique electronic properties such as high electron mobilities, tunable band structures, high thermal conductivity & topological protected states.
- Improved current device technology. Transport & topological properties suitable for spintronic devices and quantum computing.

□ Applications of 2D materials

- Optoelectronics (Photodiodes, LED's etc.,)
- FET's
- Topological insulators
- Thermoelectrics
- Spin & Valley-tronics
- Catalysts
- Chemical & biological sensors

□ Carbon Nitride Films:

○ Properties:

- Higher Hardness
- High transparency
- Chemical inertness

○ Applications:

- Hard transparent optical coatings
- Wear resistant coatings
- Semiconductor material

Background and Motivation (Cont'd.,)

□ Structure/Nomenclature of Organic Compounds

- Triazine ($C_3N_3H_3$) units and tri-s-triazine (C_6N_7) units – Heptazine, constitute allotropes of $g-C_3N_4$, differing in stability due to different electronic environment of nitrogen atoms and the sizes of nitride pores.
- Melamine: $C_3N_6H_6$: Derivative of 1,3,5-triazine (s-triazine).
- Melam: $C_6N_{11}H_9$: Obtained by condensation of melamine.
- Melem: $C_6N_{10}H_6$: Obtained by polymerization of melamine. (Compound with 3 amino substituents 2,5,8-triamino-tri-s-triazine)

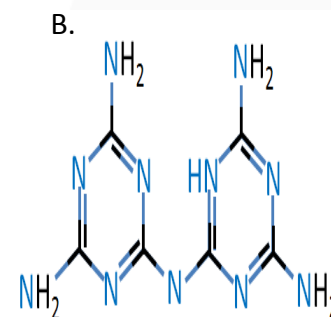
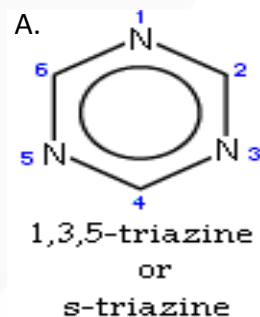


Fig. A. 1,3,5 – triazine (s-triazine), Source: “Wiki ”.
B. S-Triazine unit based structure model of potential $g-C_3N_4$ allotropes [3].

□ Melon: $g-C_3N_4$:

- Most stable allotrope, that complements carbon in materials.
- High local crystal packing. Carbon like 2D material. Comprises a 2D sheet of carbon and nitrogen atoms.
- A polymeric derivative. Heptazine ($C_6N_7H_3$) polymerized with tri-s-triazine (C_6N_7) units through an amine (link).
- Made by Berzelius and named by Liebig, is the oldest known synthetic polymer [1], [5].
- Structurally analogous to carbon only graphite.

□ Dicyandiamide (Dicy): $C_2N_4H_4$:

- Organic chemical, also called 2-cyanoguanidine.
- Precursor for $g-C_3N_4$. Easily accessible monomer.
- White crystal with many crystalline shapes.
- Uses:
 - Raw material in pesticides, plastics and medicine.
 - Surface hardener in steel industry.
 - As an additive in chemical fertilizer.

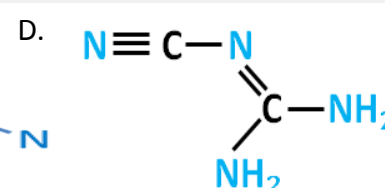


Fig. C. Mono layer graphitic Carbon Nitride ($g-C_3N_4$) named as “Melon” by Liebig dating back to circa 1834 [1].
D. Dicy Structure [2].

Background and Motivation (Cont'd.,)

□ Synthesis method for 2D materials

➤ Single-layer 2D materials:

- Most common class of crystalline structure which can be exfoliated as stable single layers are Van der Waals structure. Features of crystal structure include:
- Neutral single-atom thick or polyhedral-thick layers of atoms, covalently or ionically connected with neighbors within each layer.
- Layers are held together via Van der Waals bonding along the third axis.
- Weak interlayer Van der Waals energies ($\approx 40\text{-}70\text{ meV}$) enable facile layer exfoliation.
- Common approach to obtain single & few-layer thick 2D materials from these solids include mechanical exfoliation of large crystals (using “Scotch tape” approach [8](#)).

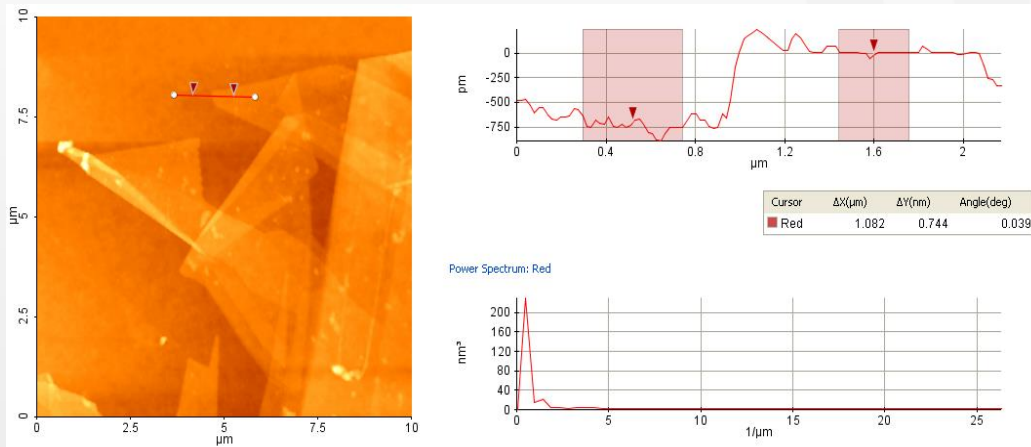


Fig. 1. AFM image of Graphene [3].

Figure 1:

- AFM image of graphene transferred to Si wafer coated with 90 nm of oxide by mechanical exfoliation process via non-contact mode.
- The red line across the edge of graphene on AFM image, is height profile.
- The step height at the edge of the graphene is about 0.744 nm, measured by inserting a pair of red cursors, as shown in top right corner of Fig. 1.

Background and Motivation (Cont'd.,)

□ Characterization of 2D material

- Single & few-layer flakes on dielectric surface alter the interference, and thereby create a color contrast between flake, substrate.
- Thickness of dielectric coating is optimized to be within 5 nm of ideal values.
- As index of refraction (which is complex & varies w.r.t crystal axes) of many 2D materials is unknown, initially it is necessary to exfoliate onto different substrates with different dielectric thicknesses to determine the optimal thickness value.
- Single-layer configurations only of metal dichalcogenides (such as MoS_2 , Ws_2) have direct bandgaps, allowing to be visualized directly by fluorescence microscopy.
- But as number of layers increase, the bandgap of these materials become indirect thereby reducing their fluorescence.

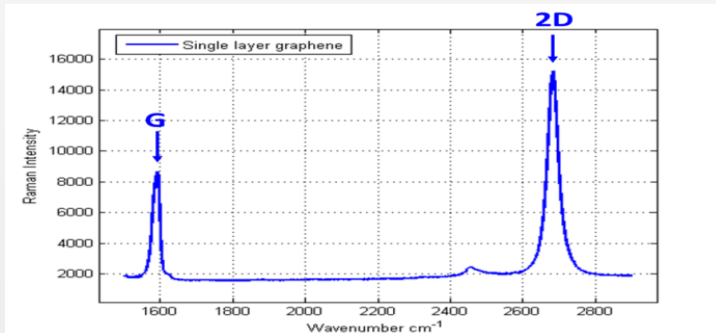


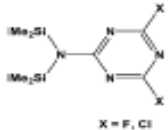
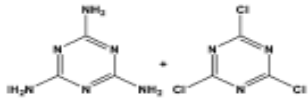
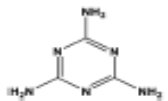
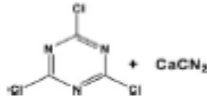
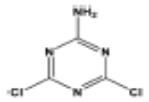
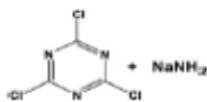
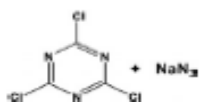
Fig. 2. Raman spectrum characterization of single layer graphene [3].

Figure 2:

- Raman spectrum of graphene transferred to silicon wafer, coated with 90 nm of oxide by CVD synthesis method, illustrating the G peak and 2D band feature characteristic of the single-layer graphene.

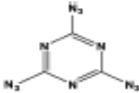
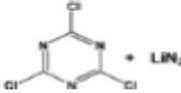
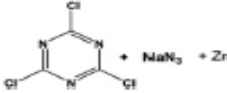
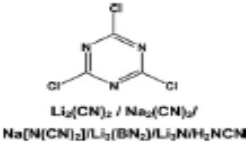
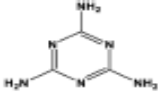
Background and Motivation (Cont'd.,)

Table 1 Some recently reported syntheses of carbon nitrides, slowly approaching the ideal g-C₃N₄ material From: "[5]".

Precursor	Conditions	T/°C	C : N ratio of the product*	Observations	Ref.
 <p>X = F, Cl</p>	Thin layer deposition (CVD)	450–500	0.81	Amorphous material	Kouvetakis <i>et al</i> 1994 (ref. 8)
	Solvothermal, in super-critical Et ₃ N (140 MPa)	250	0.81 (37 at% of H)	Slightly crystalline material	Montigaud <i>et al</i> 2000 (ref. 9)
	Solvothermal in hydrazine (2.5 GPa)	800–850	0.90 (19 at% of H)	Crystalline material	Montigaud <i>et al</i> 2000 (ref. 9)
	Solid state reaction	500–550	0.75	Crystalline material (some amounts of graphite)	Guo <i>et al</i> 2003 (ref. 10)
	Solid state reaction (1–1.5 GPa)	500–600	0.68 (7 at% of Cl)	Crystalline material	Zhang <i>et al</i> . 2001 (ref. 11)
	Solvothermal in benzene	180–220	0.72	Crystalline material	Guo <i>et al</i> 2003 (ref. 12)
	Solvothermal in benzene	220	0.80	Nanotubes	Guo <i>et al</i> 2004 (ref. 13)
(C ₆ N ₇ (NCNK) ₃) _n + C ₆ N ₇ Cl ₃ Melon CCl ₄ + NH ₄ Cl	Solid state reaction Solid state reaction Solid state reaction	300 → 600 700 400	0.71 0.67 N/A	Oligomers Crystalline material Crystalline nanoparticles	Komatsu 2001 (ref. 14) Komatsu 2001 (ref. 15) Bai <i>et al.</i> 2003 (ref. 16)

Background and Motivation (Cont'd.,)

Table 1 (Cont'd.,) From: "[5]".

	Thermal decomposition	185	0.77	Amorphous	Gillan 2000 (ref. 17)
$C_6N_7(N_2)_3$	Thermal decomposition	~200	0.83–0.71	Amorphous (rods/porous materials)	Miller <i>et al.</i> 2007 (ref. 18)
	Solid state reaction	500	0.8	Amorphous (hollow spheres)	Zimmerman <i>et al.</i> 2001 (ref. 19)
	Solid state reaction (400 MPa)	220	1.01	Crystalline (nanowires)	Lu <i>et al.</i> 2007 (ref. 20)
Melamine(dicyandiamide)	CCl_4 (4.5–5 MPa)	290	0.72	Graphite-like nanobelts and nanotubes	Li <i>et al.</i> 2007 (ref. 21)
	Solid state reaction	250–350	0.61–0.70	Micro- and nanotubes	Tragl <i>et al.</i> 2007 (ref. 22)
	Solid state reaction	350–650	0.65	Crystalline (flake-like and strip-like morphology)	Zhao <i>et al.</i> 2005 (ref. 23)
Tricyanomelaminite salts	Thermal decomposition	>450	0.66	Graphitic	Lotsch and Schnick 2006 (ref. 24)

^a The C : N ratio of ideal C_3N_4 is 0.75.

Part II

CVD growth process of single layer film of carbon nitride

☐ Thermogravimetric study of Dicyandiamide (Dicy)

• Materials & methods

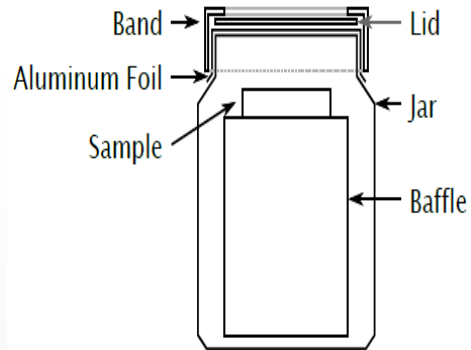


Fig. 3. Closed container for Dicy TG analysis, used in the experimental setup as shown in Fig. 4.

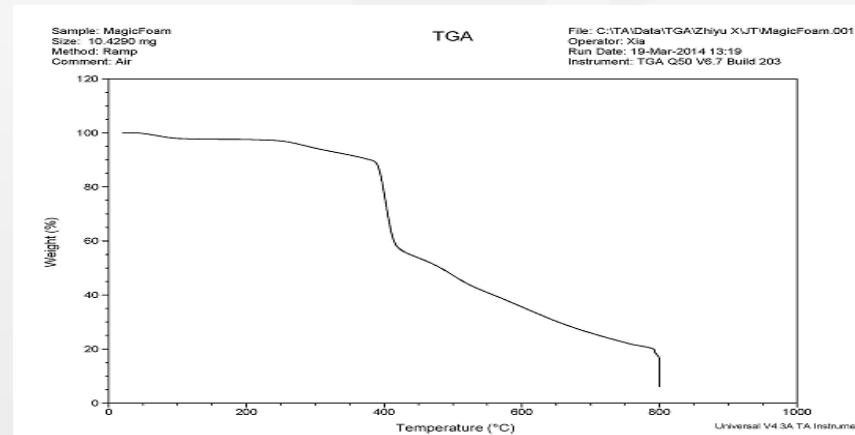
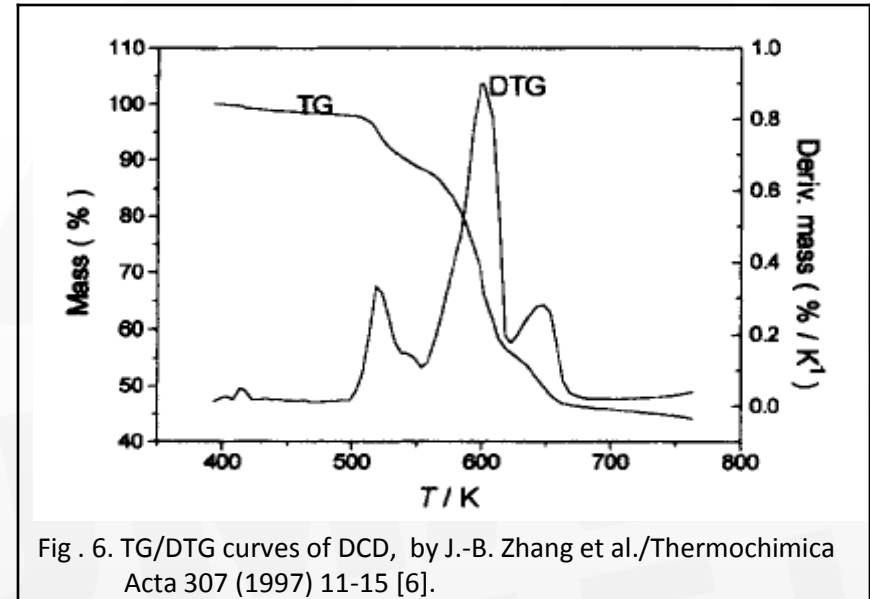
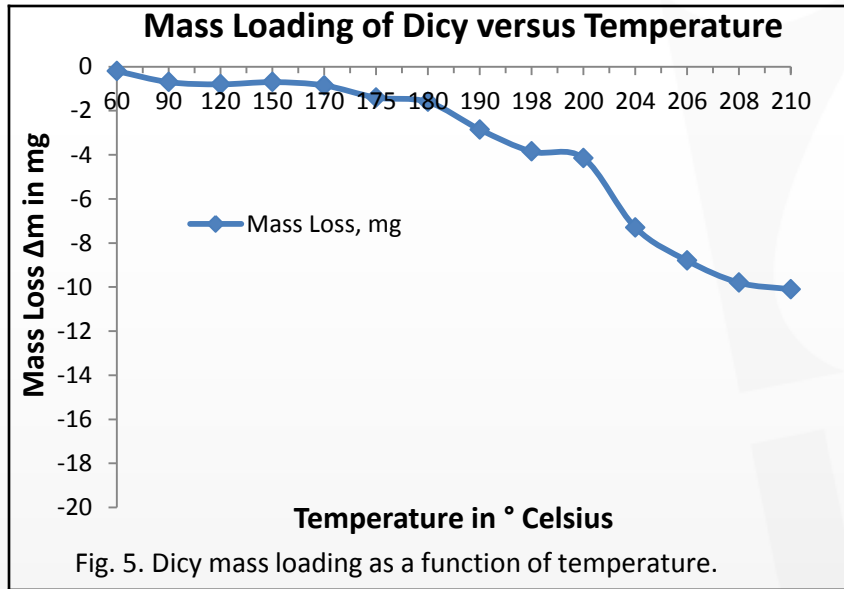


Fig. 4. Experimental setup for TG of Dicy sample measurements.

- Two sets of measurements were made with three Dicy samples in each set.
- Each measurement was made with the oven containing three sample containers, a thermocouple attached to the container surface to record sample temperature, and a thermocouple taped to the interior surface of the oven, to record oven surface temperature.
- For study in the temperature range of 200 ° C-210 ° C, the oven temperature was maintained at 200 ° C for about 30 min.
- The three samples from the previous temperatures stages were removed, while keeping the oven on & without altering the temperature knob. The first Dicy sample sets were then weighed and readings were recorded.
- The oven was then loaded with three new Dicy sample containers. The oven was left in this state for over 90 minutes, then the three containers were removed and the samples weighed. This process is repeated till sufficient data is collected, for analysis of Dicy with respect to temperature changes as shown in Fig. 5.

CVD growth process of single layer film of carbon nitride (Cont'd.,)

- Mass loading curve of Dicy w.r.t temperature versus TG of Dicy under dry nitrogen atmosphere [6] and TGA of Melamine [3].



CVD growth process of single layer film of carbon nitride (Cont'd.,)

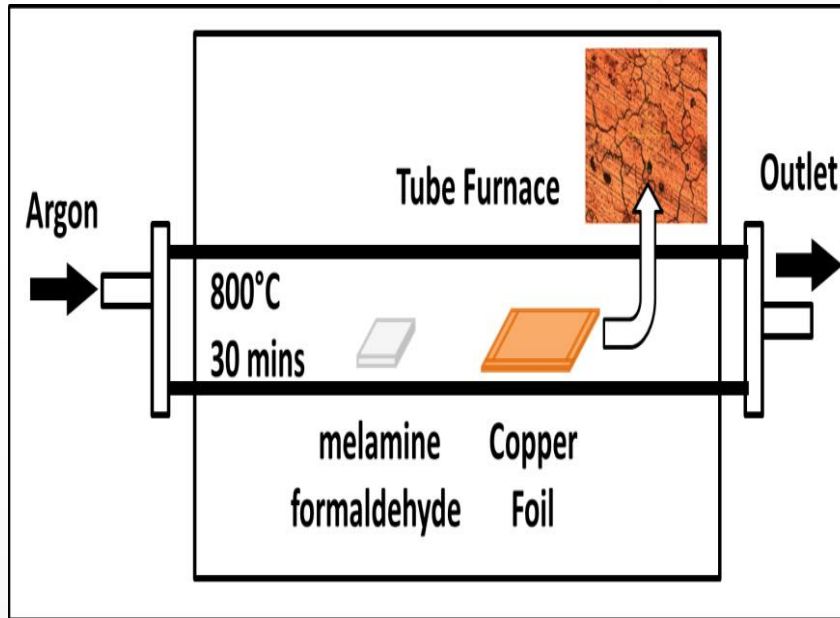


Fig. 8. Block diagram of CVD set up to synthesize 2D carbon nitride [3].



Fig. 9. CVD experimental set up for synthesis of 2D carbon nitride [3].

- At high temperatures, carbon and nitride rich solid precursor (such as Melamine-formaldehyde, rich with carbon and nitride composition), decomposes to form simple CN molecules.
- Layered carbon nitride film on the copper surface is deposited, when these molecules react chemically with copper foil (catalyst).
- CVD chamber, in the above setup is heated up to 800 °C for 30 minutes.
- During the synthesis process, Argon gas is induced into the furnace chamber .
- Image in the upper portion of Fig. 8, shows the copper surface, after synthesis is completed.

CVD growth process of single layer film of carbon nitride (Cont'd.,)

Results demonstrated by [3]

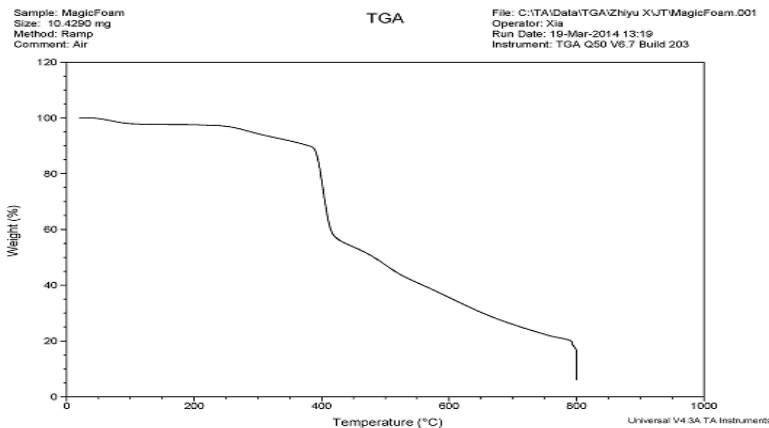


Fig. 10. For Melon Synthesis – Study of TGA curve of melamine [3].

Figure 10:

- A porcelain crucible with 0.01 gm of precursor melamine-formaldehyde is loaded into the tube furnace of Fig. 9.
- Temperature is increased from room temperature to about 800 °C at a rate of 20 °C /minute.
- An abrupt weight loss of melamine-formaldehyde occurs at 400 °C.
- As the temperature of the furnace increases further, precursor weight gradually decreases .
- Finally, when the temperature reaches 800 °C, precursor weight decreases to 0. Two abrupt weight decreases can be observed at 400 °C and 800 °C respectively.

From [3].

Figure 11:

- UV test data is processed and plotted as energy curve, shown in Fig. 11, after De-chelation process to remove iron from melon sample is performed.
- A tangential line on the energy curve, is drawn to read the energy-gap directly from the plot.
- The point of intersection of tangential line and the null intensity axis point gives the value of the band-gap of melon material.
- From the melon energy curve, 4.2 e.V is therefore the bandgap of graphitic single-layer carbon nitride.

From [3].

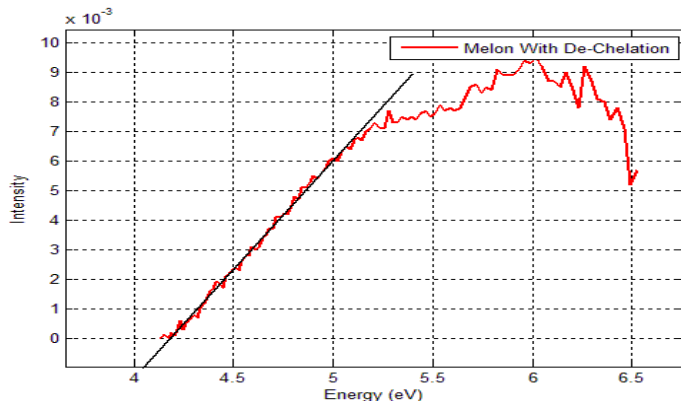


Fig. 11. Melon's bandgap energy plot [3].

CVD growth process of single layer film of carbon nitride (Cont'd.,)

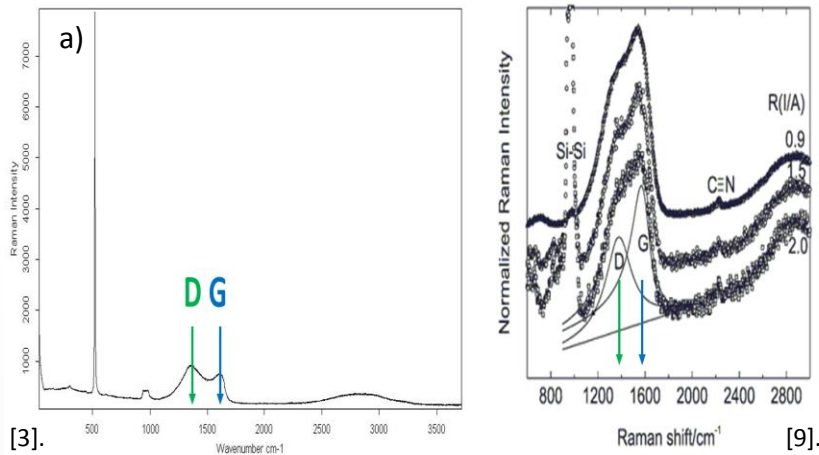


Fig. 12 a) Raman Spectrum [3].

Figure 12 a): Raman spectrum of

- Carbon nitride film prepared on Si substrate coated with 90 nm SiO₂ by CVD synthesis³.
versus
- Ion beam assisted deposition method for Carbon nitride films prepared on Si substrates⁹.
- For each of these processes, D peaks of samples are located at 1400, and G peaks of samples are located at 1600.

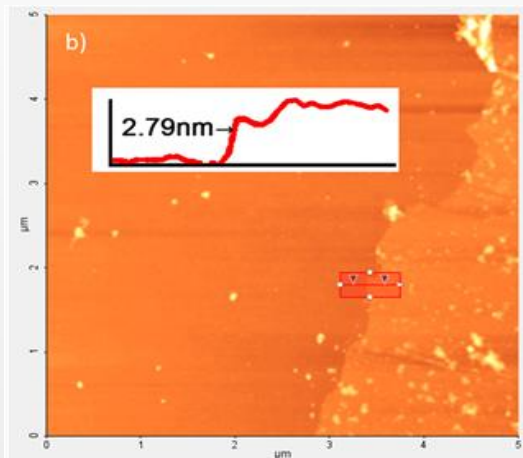


Fig. 12 b) AFM operated in noncontact mode to measure the thickness of melon [3].

Figure 12 b):

- Non-contact mode AFM image of melon transferred to silicon wafer coated with 90 nm of oxide by CVD synthesis method.
- Across the edge of melon on lower side of AFM image, height profile is shown with a red line.
- The step height at the edge of the melon is measured as 2.79 nm, by inserting a pair of red cursors.

CVD growth process of single layer film of carbon nitride (Cont'd.,)

- **Limitations**

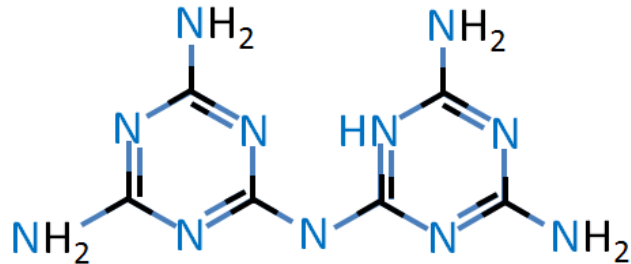


Fig. 13. S -Triazine unit based structure model of potential g-C₃N₄ allotropes [3].



Fig. 14. Mono layer graphitic Carbon Nitride (g-C₃N₄) named as "Melon" by Liebig dating back to circa 1834 [1].

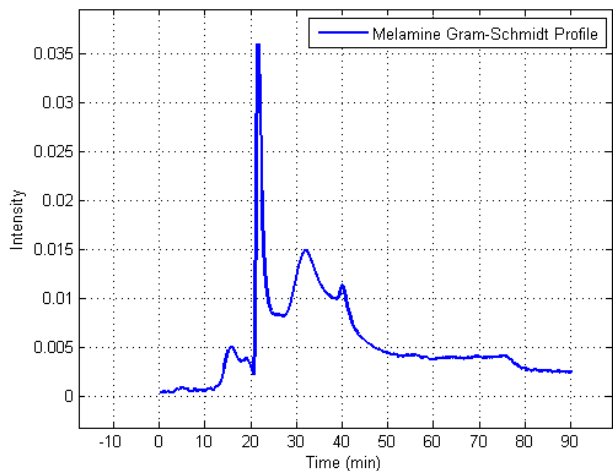


Fig. 15. FTIR Gram-Schmitz profile [3].

Figure 15. Melon¹ synthesis TGA Gram-Schmidt chart by [3]:

- Shows a peak at 20 minutes, which is the time when furnace tube temperature of Fig. 9, reaches 400 °C.
- The peak suggest that some form of chemical reactions are taking place, inside the CVD chamber unit.
- This information needs to be combined with FTIR data, in order to get more accurate details about the reactions, so as to find out what elements occur/compose the gas molecules that are present inside the CVD chamber.
- A further analysis of the FTIR data is required, if more thorough knowledge about the gas constitution inside the chamber is needed to have a controlled growth environment, which creates new challenges in the overall process scalability.

CVD growth process of single layer film of carbon nitride (Cont'd.,)

Proposed design for gas delivery system for controlled CVD growth

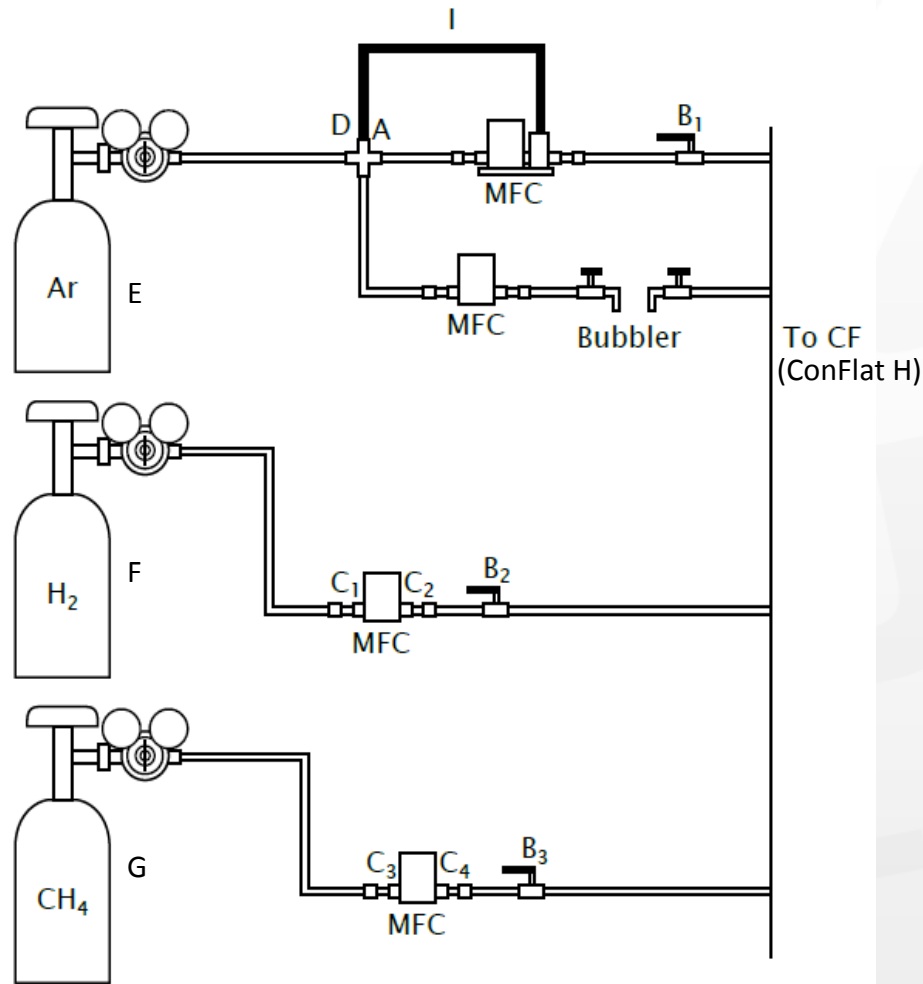


Fig. 16. Block diagram of the gas delivery system, a design for achieving a controlled and well characterized CVD growth mechanism.

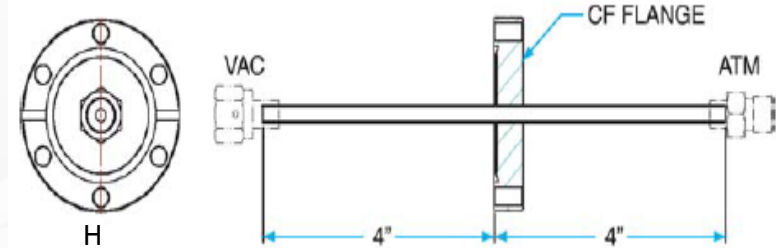


Fig. 17. Vacuum system integration with the proposed design of Fig. 16.

Table 2. Description of components depicted in Fig. 16.

Label	Description
A	Type 316 SS Yor-Lok Tube Fittings, Cross Connector, Tube-to-tube, 1/4"
B ₁ , B ₂ , B ₃	Type 316 Stainless Steel Ball Valves with Yor-Lok Fittings, Lockable Lever, 1/4"
C ₁ , C ₂ , C ₃ , C ₄	Type 316 SS Welded VCR Face Seal Fitting, Swagelok Tube Fitting Connector, 1/4 in. WVCR x 1/4 in. Tube Fitting, Swagelok Fittings
D	Type 316 Stainless Steel Yor-Lok Tube Fittings, Tube Support, 1/4" OD 1/8" ID
I	Low-Pressure Polypropylene Semi-Clear Tubing, 1/4" (Units of 25', 50', 100' per foot)

CVD growth process of single layer film of carbon nitride (Cont'd.,)

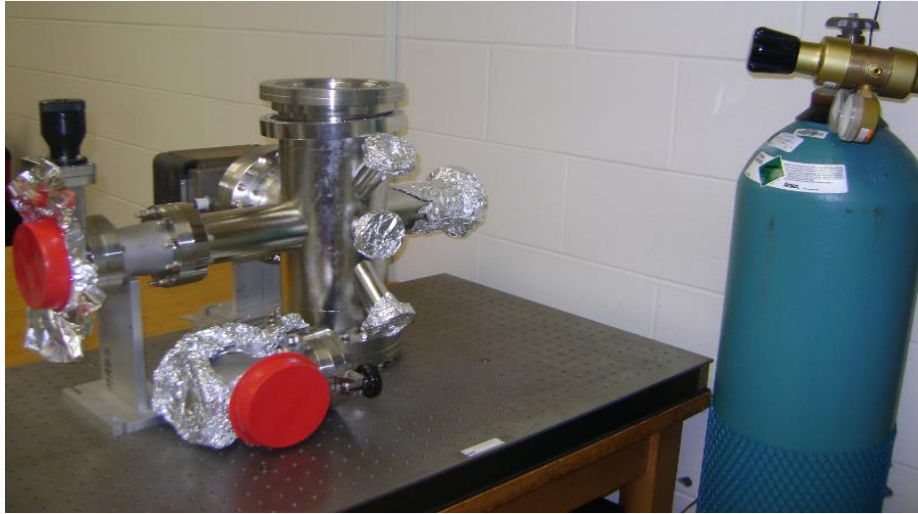


Fig. 18. Partial experimental setup of the vacuum system as shown in Fig. 17, for CVD growth of single layer g-C₃N₄ films.



Fig. 19. Top view of the Vacuum sub-system chamber, with various connection ports, for deployment in CVD process.



Fig. 20. Mass flow controllers, Flow meter by mks as depicted in Fig. 16, of the proposed gas delivery system .



Fig. 21. Side view of the Vacuum sub-system, showing the chamber loading door and gas inlet nozzles.

Part III

Conclusion

❑ Device Applications using 2D materials & Future Work

- Application: FET Device by [3]

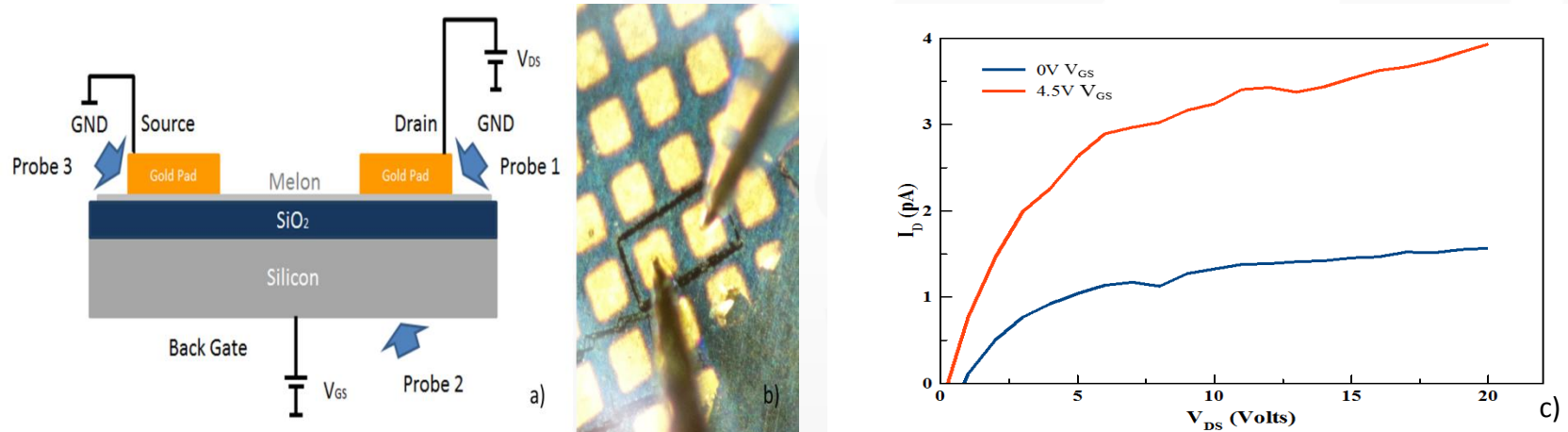


Fig. 22 a), b) Melon transistor device prepared with melon sitting on Si wafer coated with 90 nm SiO_2 insulation film, and c) Melon FET device IV curve, showing FET behavior by responding to changes in gate voltage [3].

Figure 22.

- Melon FET diagrams with Source and Drain connected to gold electrodes, and drain connected to Si substrate in the back.
- Physical /Practical melon FET device, which is prepared on Si substrates coated with 90 nm thick SiO_2 film where the top gold electrodes are prepared by physical vapor deposition method.
- Drain current (I_D) versus drain to source voltage (V_{DS}) at increasing gate voltages (V_{GS}). Drain-source IV curve with 0 V gate to source bias voltage is shown with blue in fig. c). Drain-source IV curve with 4.5V gate to source bias voltage is shown with red in fig. c).

□ Future Work

• (1). Optoelectronics: Photodetectors using 2D materials.

Photosensing system capable of detecting light spanning from IR to UV regimes.

Goal: Photodetectors using mono layer thick graphitic Carbon Nitride ($g\text{-C}_3\text{N}_4$) material grown with the proposed CVD.

- To minimize the leakage current & maximize responsivity of this photodiode.
- Solarblind UV Photodetectors.

From [10].

- Responsivity $R = \frac{\text{Generated Photocurrent (A)}}{\text{Incident Optical Power (W)}} = \frac{I_p}{P_o} = \frac{\eta q}{h\nu}$

where η is the Quantum efficiency, $\eta = \frac{\text{Number of free EHP generated and collected}}{\text{Number of incident photons}} = \frac{I_p/q}{P_o/h\nu}$ and

$E_p = h\nu = hc/\lambda$, is the photon energy.

- Photocurrent $I_p = RP_o$, where P_o is the incident power on the photodetector.
- Dark Current: It is the current flowing in absence of an optical signal. Generated in the bulk of device due to random generation of EHP's. Dark current results in leakage current, that flows across the surface of p-n junction devices.
- Leakage Current: Caused by the noise generated by leakage current along the surface.
(Not from the bulk of device).
- (2). **Materials Science: Ferrous and non-ferrous metals and alloys** (carbon steels alloy, die steels & tool sets).
Compounds of Carbon, Boron Nitride polymorphs, for ferrous metal polishing and fast cutting ferrous alloys, because of their similar atomic sizes and structures.

Acknowledgement

This is a joint effort of an ongoing academic research work at UML via university faculty directed research proposal at the Mark and Elisia Saab Emerging Technologies and Innovation Center (ETIC). The authors thank UMass Lowell ECE Dept. and all the mentioned centers for their contributions in permitting us to avail their facilities, during course of our research work. Further research project information can be obtained by contacting the following:

- ▶ 1. Prof. Joel Therrien Ph. D, Professor, ECE Department, BL 319, UMass Lowell.
- ▶ 2. UMass Lowell, ECE Dept., 1 University Ave., Ball Hall 301, Lowell, MA 01854

References

- [1]. J. Liebig, *Annalen*, 1834, 10, 10.
- [2]. E.W. Hughes, *J. Am. Chem. Soc.* 62 (1940) 1258.
- [3]. Yancen Li, "MELON – A 2D Material beyond Graphene," UMass LOWELL Dissertation, ECE Dept., 2015.
- [4]. Butler *et al.*, "Progress, Challenges, and Opportunities in Two-Dimensional Materials Beyond Graphene," *ACS NANO* 2013, Vol. 7, No. 4, 2898–2926, (2013 American Chemical Society).
- [5]. Arne Thomas, Anna Fischer, Frederic Goettmann, Markus Antonietti, Jens-Oliver Muller, Robert Schlogl and Johan M. Carlsson, "Graphitic carbon nitride materials: variation of structure and morphology and their use as metal-free catalysts," *J. Mater. Chem.*, 2008, 18, 4893–4908 | 4893 The Royal Society of Chemistry 2008 – Max-Planck-Society/Max Planck Institute of Colloids and Interfaces.
- [6]. Ji-Biao Zhang, Zhi-Cheng Tan, Shuang-He Meng, Shao-Hui Li, and Li-Ming Zhang, "Heat capacity and thermal decomposition of dicyandiamide," *Elsevier Thermochemica Acta* 307 (1997) 11-15
- [7]. Algara-Siller G, Severin N, Chong SY, Björkman T, Palgrave RG, Laybourn A, *et al.*, "Triazine-Based Graphitic Carbon Nitride: A Two-Dimensional Semiconductor," *Angewandte Chemie Int'l.* ed. 2014, 53, 7450-7455.
- [8]. Muingsheng Xu, Tao Liang, Minmin Shi, and Hongzheng Chen, "Graphene-Like Two-Dimensional Materials," *American Chemical Society Journal*, [dx.doi.org/10.1021/cr300263a](https://doi.org/10.1021/cr300263a), *Chemical Reviews* July 2012.
- [9]. Sucasaire W, Matsuoka M, Lopes KC, Mittani JC, Avanci LH, Chubaci JF, *et al.*, "Raman and infrared spectroscopy studies of carbon nitride films prepared on Si (100) substrates by ion beam assisted deposition," *Journal of the Brazilian Chemical Society* 2006, 17(6): 1163-1169.
- [10]. Gerd Keiser, "Optical Fiber Communications," *Photodetectors*, Chapter 6, 4th Edition, 2012 Tata McGraw Hill.

THANK YOU

